NASA/TM–2020-5005041

Calibrating a 3-Axis Accelerometer Instrument with a Less Accurate Calibration Device Part 1: Mathematical Methodology.

Hector L. Soto
Langley Research Center, Hampton, Virginia

August 2020

NASA STI Program . . . in Profile

Since its founding, NASA has been dedicated to the advancement of aeronautics and space science. The NASA scientific and technical information (STI) program plays a key part in helping NASA maintain this important role.

The NASA STI program operates under the auspices of the Agency Chief Information Officer. It collects, organizes, provides for archiving, and disseminates NASA's STI. The NASA STI program provides access to the NTRS Registered and its public interface, the NASA Technical Reports Server, thus providing one of the largest collections of aeronautical and space science STI in the world. Results are published in both non-NASA channels and by NASA in the NASA STI Report Series, which includes the following report types:

- TECHNICAL PUBLICATION. Reports of completed research or a major significant phase of research that present the results of NASA Programs and include extensive data or theoretical analysis. Includes compilations of significant scientific and technical data and information deemed to be of continuing reference value. NASA counter-part of peer-reviewed formal professional papers but has less stringent limitations on manuscript length and extent of graphic presentations.

- TECHNICAL MEMORANDUM. Scientific and technical findings that are preliminary or of specialized interest, e.g., quick release reports, working papers, and bibliographies that contain minimal annotation. Does not contain extensive analysis.

- CONTRACTOR REPORT. Scientific and technical findings by NASA-sponsored contractors and grantees.

- CONFERENCE PUBLICATION. Collected papers from scientific and technical conferences, symposia, seminars, or other meetings sponsored or co-sponsored by NASA.

- SPECIAL PUBLICATION. Scientific, technical, or historical information from NASA programs, projects, and missions, often concerned with subjects having substantial public interest.

- TECHNICAL TRANSLATION. English-language translations of foreign scientific and technical material pertinent to NASA's mission.

Specialized services also include organizing and publishing research results, distributing specialized research announcements and feeds, providing information desk and personal search support, and enabling data exchange services.

For more information about the NASA STI program, see the following:

- Access the NASA STI program home page at http://www.sti.nasa.gov

- E-mail your question to help@sti.nasa.gov

- Phone the NASA STI Information Desk at 757-864-9658

- Write to:
  NASA STI Information Desk
  Mail Stop 148
  NASA Langley Research Center
  Hampton, VA 23681-2199

NASA/TM–2020-5005041

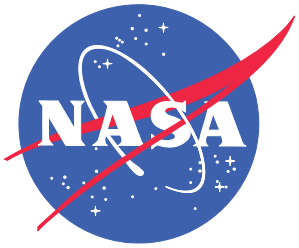

Calibrating a 3-Axis Accelerometer Instrument with a Less Accurate Calibration Device Part 1: Mathematical Methodology.

Hector L. Soto
Langley Research Center, Hampton, Virginia

National Aeronautics and
Space Administration

Langley Research Center
Hampton, Virginia 23681-2199

August 2020

Table of Contents

List of Figures

List of Tables

Nomenclature

Abbreviations

CD	calibration device (two-axis rotary system)
KM	kinematics model
RB	rigid body in the local frame of reference O*xyz*
SL	surface level

Symbols

b	Roll of the full system (as a rigid body)
a	Average pitch misalignment = *a*1 + *a*2 + *a*3
*a*1	Pitch of the full system (as a rigid body)
*a*2	Pitch Table index misalignment
*a*3	Pitch misalignment of the small table attachment
d	Average orthogonality misalignment between rotary device
*d*1	Yaw wobble from the pitch table
*d*2	Yaw misalignment between the two rotary devices
e	Average pitch of the *x*-*y* plane = *e*1 + *e*2
*e*1	Pitch wobble from the roll table
*e*2	Pitch misalignment of the interface *x*-*y* plane
f	Average roll misalignment = *f*1 + *f*2 + *f*3 + *f*4
*f*1	Roll wobble from the pitch table
*f*2	Roll misalignment of the small table attachment
*f*3	Roll Table index misalignment
*f*4	Roll misalignment of the interface *x*-*y* plane
k	Average yaw of the *x*-*y* plane, = *k*1 + *k*2
*k*1	Yaw wobble from the roll table
*k*2	Yaw misalignment of the interface *x*-*z* plane
p	Pitch angle, calibration first rotary device articulation of the *x*-*y* plane
r	Roll angle, calibration second rotary device articulation of the *x*-*y* plane
yfb	Orientation of the *x*-*z* plane alignment with *x* sensor pointing forward or backwards
utb	Orientation relative to the *x*-*y* plane, mount on top or bottom
B	Instrument Bias vector
S	Instrument Sensitivity matrix
O*xyz*	Local coordinate frame
O*XYZ*	Global coordinate frame
G	projected RB rotations to the Global frame of reference O*XYZ*
Gwg	Global frame of reference with gravity (g) in the –*Z*-axis
x	*x*-axis local coordinate frame
y	*y*-axis local coordinate frame
z	*z*-axis local coordinate frame
X	*X*-axis Global coordinate frame
Y	*Y*-axis Global coordinate frame
Z	Z-axis Global coordinate frame
g	gravity

g*v*	Instrument local frame projected on the global frame Gwg
*p*rot	3D pitch rotation
*r*rot	3D roll rotation
*y*rot	3D yaw rotation

Abstract

A three-axis accelerometer instrument (3xAI) can provide the angular attitude of a 3D object using the gravity vector (g) as the sole reference. Calibrating such an instrument requires placing it at known (to some accuracy plus uncertainty) angular articulations with respect to g. This paper will show a potential process for calibrating a 3xAI by using a 2-axis rotary system (calibration device) to provide these articulations. Any calibration device (CD) with such capacity will contain internal misalignments. These misalignments, even if made relatively small or approximated to zero in the kinematics model (KM), can be detrimental to the calibration of the instrument when high measurement accuracy is required. This is especially true if the selected set of articulations chosen for calibration do not include their symmetrical counterpoints (a point where the misalignment has equal magnitude but is opposite in direction to a point chosen). The consequence of not including the combination, point and counterpoint, for any misalignment involved in the calibration, results in a biased instrument. This paper will demonstrate a calibration of the instrument using symbolic math resulting in a closed-form solution of the instrument coefficients. The main objective is to show the impact of all the CD misalignments to the instrument coefficients. This process is the basis for a more sophisticated method (shown in a future paper) for obtaining the instrument coefficients while simultaneously obtaining an estimate of the calibration device internal misalignments.

1.0 Introduction

The aeronautics research community relies on angle measurements for a multitude of applications for all wind tunnel tests. Angle measurements are used for model build up and installation, sting bending estimates, and to calibrate any angle of attack or model pitch attitude device used during wind-on conditions. A single axis gravity referenced instrument can be used to achieve most of the angle measurement needs that support these tests. Recently, with the development of the 3xAI instrument, which provides the capability of measuring pitch and roll simultaneously, this instrument has been favored when applicable over single axis instruments in all NASA wind tunnel facilities.

To calibrate this instrument to high accuracy requires a CD that can provide known inputs to an accuracy that is higher than that for the instrument. Although this is standard practice in all things metrology, it is very challenging to perform for this instrument. NASA has developed a CD to accomplish this but not without overcoming some major challenges. These challenges are that the system is in alignment with the gravity vector and that all rotations and angle articulations relative to this reference (gravity) are known to high accuracy. To manufacture such system and guarantee these results is not an easy task. Any system which provides pitch and roll angle articulations will contain a number of internal misalignments that are nearly impossible to zero out. For this reason, a number of procedures were developed to align the system with gravity and therefore increase the confidence level of system accuracy. Even with this increased confidence level, the small internal misalignments within the system can still have an impact on the instrument calibration coefficients, especially for instruments with higher accuracy needs. In other words, for low accuracy instruments this may not be an issue, but for higher accuracy ones this may be detrimental to improving measurement accuracy.

To alleviate this issue, a goal to measure these internal misalignments within the system was attempted using state of the art instruments. Unfortunately, this was not successful due to some of the locations of these misalignments within the system and their very small magnitude. The other misalignments could only be measured relative to a different reference, other than gravity. The accuracy of this approach did not meet the stated requirements.

In order to solve this problem it required a new approach to understand how these misalignments could impact the instrument calibration coefficients if we have no knowledge of their magnitude and direction. The following sections of this paper will show an approach developed to observe this impact. One outcome from this work is that it is possible to cancel the effects of these misalignment within the coefficients of the instrument. This is only possible if the CD that produces these inputs to the instrument during calibration meets a number of assumptions specified in Section 2.

The process for calibration of a three-axis accelerometer instrument (3xAI) can be very similar to the process for calibrating a single axis tilt sensor if you can overcome some challenges. One of these challenges is having a mathematical model for the instrument that lends itself to leverage this method. In this paper an ideal math model, shown in Section 3, for the instrument is chosen to simplify this pseudo derivation of the instrument calibration.

The process to calibrate a single axis sensor requires a clean, flat, and near-level surface and two readings, see Figure 1. First you place the instrument on the surface in any random orientation and take the first reading R1 (look at Figure 1 on the right side if the Z vector and the lines above the black line, which represent the first orientation of the single axis sensor; R1 = SL + e). Then, rotate the instrument exactly 180° from the original position, with respect to the surface normal vector, *z*-axis, and take the second reading R2 (it is the line below the black line, which represents the second orientation or the 180° rotation with respect to the z-axis; R2 = –SL + e. In matrix form the solution is:

Solution:
$$\begin{bmatrix} R1 \\ R2 \end{bmatrix} = \begin{bmatrix} 1 & 1 \\ -1 & 1 \end{bmatrix} \begin{bmatrix} SL \\ e \end{bmatrix} \rightarrow \begin{bmatrix} SL \\ e \end{bmatrix} = \begin{bmatrix} \frac{1}{2} & -\frac{1}{2} \\ \frac{1}{2} & \frac{1}{2} \end{bmatrix} \begin{bmatrix} R1 \\ R2 \end{bmatrix} \quad (1)$$

This procedure takes advantage of symmetry and the instrument's sensitivity to the local gravity vector rather than the surface used. The surface used is just the means to provide a stable and repeatable position to the inclinometer relative to the gravity vector (g). This procedure gives both the instrument error (offset angle), e, and an estimate of the surface angle, SL, with respect to level (defined in this paper as a misalignment). The surface misalignment with respect to level is the delta between the readings divided by 2, and the instrument error is the sum of the readings divided by 2.

Leveraging this process to calibrate a 3xAI is challenging because it is necessary to provide a specific set of angular articulations that contain all or some of the misalignments within the calibration device (CD). Each individual articulation will be an angular attitude in 3D space where it maximizes the value of one or more misalignments while minimizing the rest. In addition, these

articulations shall include the symmetrical counterpoint to each angular attitude. Achieving symmetry requires an unconventional approach, which has to do with increasing the number of mounting orientations from two (shown for the single-axis calibration) to four. All articulations will be with respect to g, thus copying the procedure demonstrated above for the single-axis unit.

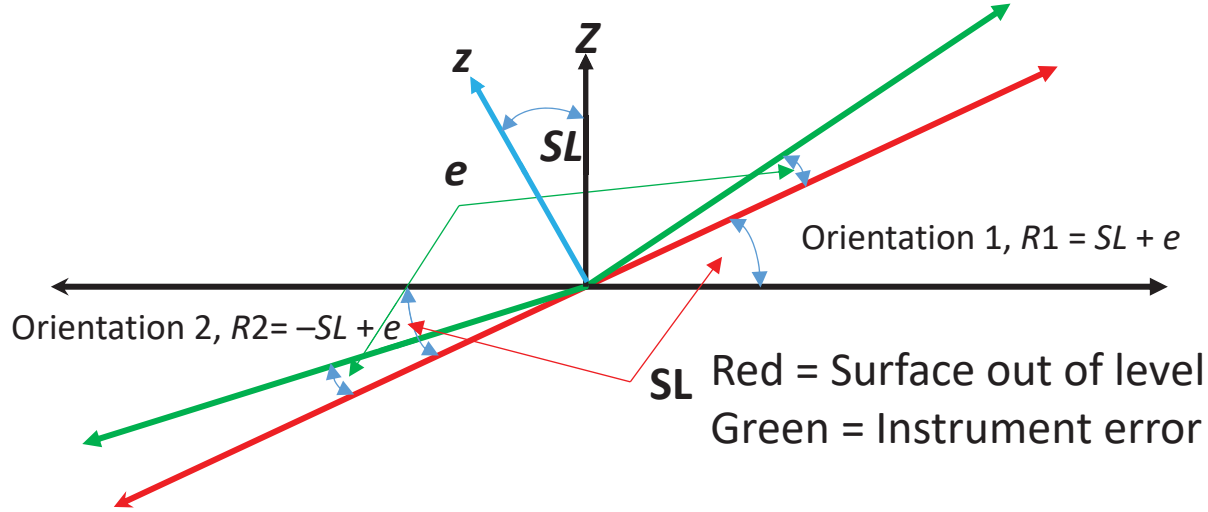

Figure 1: The black line represents a perfect horizontal level, or zero g, the red line represents the surface level, and the green represents the instrument measurement error for the two orientations measured. The angle between the red and black lines is represented by *SL*, and *e* (offset angle or error) is the angle between *SL* and instrument sensor. Upper case *Z* (–*Gwg*, global frame with gravity) is the normal vector to the black line and the lower-case *z* is the normal vector (shown in blue) to the red line.

2.0 Assumptions:

To demonstrate this work, it is important to stipulate a few assumptions about the calibration device and instrument:

1. The calibration device has a determinable number of internal misalignments. Although this paper will not provide an estimate for any of these values, it will show the quantitative effects they have on the instrument coefficients.
2. The values of these internal misalignments are not known for this demonstration, but they are assumed to be within +/- 0.5°. Then again, based on the single-axis calibration procedure (where surface level (SL) is not known), exact values are not required.
3. The misalignments in the calibration device never change during the calibration process. If they happen to vary, then they are assumed to be sinusoidal or random with a zero average.
4. The calibration device provides the exact corresponding symmetrical articulation during the calibration. This applies to the four mounting orientations required for this process explained in Section 5.
5. The calibration device will have two interface planes represented by the *x*-*y* plane and *x*-*z* plane. The assumption here is that these planes are flat, smooth, and near identical for all mounting orientations. See Section 4 for illustration.

6. The calibration device global frame is in alignment with the global frame that contains gravity, Gwg, in the *Z*-axis. More details found in the description of the calibration device (Section 3.2).
7. Each sensor in the instrument has a zero bias (i.e., electrical bias or the voltage output of the sensor when oriented with the zero-g field).
8. The sensitivity of each sensor is 1 Volt per g (1 Volts/g).
9. The sensors are sensitive enough to observe the calibration device articulations including the misalignments.
10. The three sensors are orthogonal to each other, with the *x*-axis and *y*-axis sensors forming the *x-y* interface plane and the *x*-axis and *z*-axis sensors forming the second interface plane (see Figure 2). These planes pertain to the instrument and are used to align the instrument to the calibration device or test article.

These assumptions are not specifically obvious, and they are challenging to duplicate with a real physical calibration system and instrument. If these assumptions do not hold, then it will be challenging to calibrate this instrument without biasing it.

3.0 Description and Math Model for the Instrument and the Calibration Device

3.1 The 3-Axis Accelerometer Instrument (3xAI)

The real physical instrument in Figure 2, 3xAI, is composed of three servo-accelerometers placed orthogonally in a structural frame. This frame will contain the two interface planes as described in assumption 10. The first plane attaches to the object of interest; it has three feet and fastener holes placed at the base of the frame. Two dowels placed on the *x*-axis of the instrument form the *x-z* plane, which aligns the instrument with the object of interest's local *x*-axis.

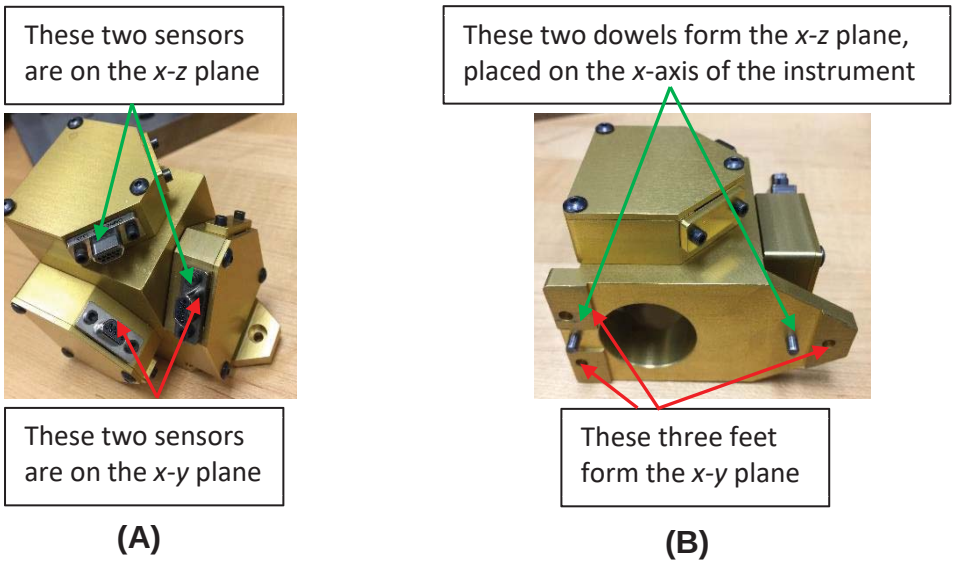

Figure 2: The real physical instrument. (A) shows the sensors positions; (B) shows the two interface planes relative to the *x-y* and *x-z* planes.

It is nearly impossible to place the three accelerometers orthogonally and aligned with both the *x-y* and *x-z* planes of the structural frame due to their sensing element alignment relative to the physical construction or mounting reference. For this reason, this instrument has been modeled using different approaches [1,2]. The method of calibrating the instrument in Reference 1 requires a non-linear least square approach found in Reference 3. In this paper, the instrument model borrows from the approach in Reference 2, but it assumes it is an ideal instrument (see assumptions 7 and 8 for a description, or to summarize them, Equation 2).

$$\begin{bmatrix} Be & Bh & Bv \\ Sexx & Shyx & Svzx \\ Sexy & Shyy & Svzy \\ Sexz & Shyz & Svzz \end{bmatrix} = \begin{bmatrix} 0 & 0 & 0 \\ 1 & 0 & 0 \\ 0 & 1 & 0 \\ 0 & 0 & 1 \end{bmatrix} \tag{2}$$

The ideal model for the instrument is represented in equation 2. The *B* is the bias, and the *S* is the sensitivity. The *e*, *h*, and *v* column vectors pertain to the individual sensors, with *e* aligned with the *x*-axis, *h* with the *y*-axis, and *v* with the *z*-axis. The main sensitivity for each sensor is the diagonal of the lower 3x3 matrix. The off diagonal sensitivities refer to the sensors' sensitivity to the other two orthogonal axes. The matrix on the right represents the numeric value of this ideal instrument.

The output of the sensor is in Volts, thus the label *V*. Then dropping the *e*, *h*, and *v* and using the appropriate axes' labels,

$$V = \begin{bmatrix} V_x \\ V_y \\ V_z \end{bmatrix};\ B = \begin{bmatrix} B_x \\ B_y \\ B_z \end{bmatrix};\ g_v = \begin{bmatrix} g_{x.Z} \\ g_{y.Z} \\ g_{z.Z} \end{bmatrix}; S = \begin{bmatrix} S_{xx} & S_{yx} & S_{zx} \\ S_{xy} & S_{yy} & S_{zy} \\ S_{xz} & S_{yz} & S_{zz} \end{bmatrix} \tag{3}$$

The instrument local frame of reference projected onto the global frame of reference containing g is equal to g_v. The instrument is sensitive to tilts relative to the global *Z*-axis (*x.Z*, *y.Z*, and *z.Z*) (Figure 3). Therefore, any linear movement (e.g., up, down, left, right, forward, or backwards) or rotations with respect to the global *Z*-axis will not change the output of the instrument.

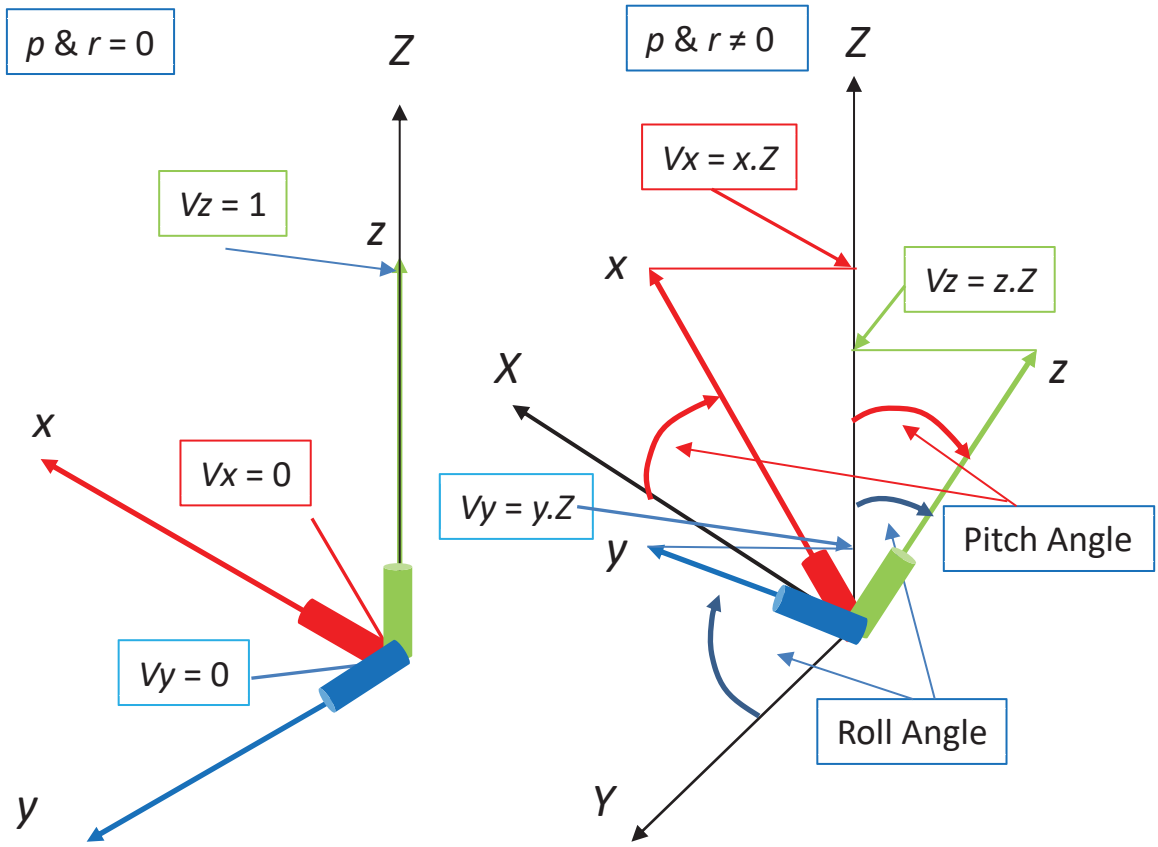

(A) **(B)**

Figure 3: The results of rotating the instrument through an angle pitch (*p*) and roll (*r*) with respect to the global frame of reference. (A) shows the ideal instrument local frame of reference in alignment with the global frame of reference. (B) shows the instrument local frame rotated in pitch and roll with respect to the global frame, and the output of the sensors as the dot product of the sensor axis with the global *Z*-axis.

The instrument output mathematical model in Reference 2 is shown as

$$V = B + g_v^T S \tag{4}$$

The angular attitude of the instrument is obtained with

$$g_v = (V - B)^T S^{-1} = [g_{x.Z} \quad g_{y.Z} \quad g_{z.Z}] \tag{5}$$

To obtain the angular attitude, the conversion from g_v to pitch and roll is

$$pitch\ angle = \sin^{-1}[g_{x.Z}] \tag{6}$$

$$roll\ angle = \arctan2\left[\frac{g_{y.Z}}{g_{z.Z}}\right] \tag{7}$$

The procedure to obtain B and S using a least square approach, found in References 2 and 4, is included in the calibration procedure shown in Section 5.

3.2 Calibration Device

The physical device is composed of two rotary index divider heads assembled to provide rotations to the instrument relative to gravity in the sensitive planes, pitch and roll. Each head has a 360° rotation range and 1° minimal increment. The articulation error (index error) for each table is considered small but repeatable and within ±2 arcsecs with uncertainty. In addition, it is assumed to have a sinusoidal pattern with zero average. The assumption for the random error component for any articulation is that it is small relative to the index error. For instance, for a pitch rotation, p,

$$p = p_i + Index\ error + random\ error$$

$$Index\ error \gg random\ error$$

where p_i is the selected integer pitch rotation number.

It is challenging to design and build a two-axis rotary system with no internal misalignments (see Figure 4 to observe the number of misalignments identified within the system used for this work). Therefore, due to this challenge, it is important to find methods that can assist with either making these misalignments near zero or determining them to a very high accuracy. A number of procedures intended to make the misalignment near zero have had some success. Unfortunately, as of today, there are no known methods to validate these procedures, and determining these misalignments has been difficult, even using state-of-the-art instrumentation. However, it is possible to estimate the internal misalignments for this device using the system as a whole (instrument and CD together). This will be the subject of a future paper.

Each rotary table can be calibrated as an individual unit following a calibration procedure similar to National Institute of Standards and Technology (NIST)-documented ones [5,6]. Unfortunately, after assembling the system, there are no known procedures to determine the articulations' accuracy with uncertainty of the CD as one system. One specific procedure developed to align the unit with the gravity vector was implemented to provide some confidence in the system alignment. This procedure is based on the idea that it is difficult to get a level plane at two symmetrical points in space. In other words, the hypothesis here is that if the system is near level (the *x*-*y* plane leveled in both the *x*-axis and *y*-axis) at two set-points, 0° pitch and 0° roll, and at 180° pitch and 180° roll, then the internal misalignments in the CD must be small. This hypothesis has been difficult to prove, mathematically or with other validation techniques. In addition, the devices (e.g., a high-accuracy bubble level, or electronic level) used to perform this leveling of the *x*-*y* plane/surface have a larger footprint relative to the instrument under calibration. Consequently, these devices can only provide an average of the mounting surface, which is not exactly the same surface area that the instrument (3xAI feet interface to the *x*-*y* plane) interfaces to. If the surface is convex or concave in the area of interest, then these devices will impart an error when leveling this plane with such external devices.

In theory, with a mathematical model for this calibration device and knowledge of the misalignment magnitude and direction, it is possible to adjust the g vector for each rotational position in space. Unfortunately, this is not as easy as it sounds. There are challenges in obtaining accurate angular positions with any device; see Section 7.6 for a description of these challenges.

The kinematics/mathematical model for this device (Figure 4) is derived from the path taken to include all of the components in the system. This path can make the math equation very large if each individual misalignment becomes a separate rotation in the equation. The approach used [7], includes the two rotation devices and a minimum of 14 misalignments (if assumptions 3.3 and 3.5 hold). If they do not hold, then the misalignments that pertain to the two interface planes (pitch, roll, and yaw) can potentially turn into 12 (one set of 3 misalignments for each mount), thus making it harder to determine the impact of these misalignments to the instrument calibration.

The path chosen groups these misalignments into a total of six groups, plus the two rotation devices. Of these six misalignments, three refer to the two interface planes (*x*-*y* and *x*-*z*). Of the remaining three, two refer to the calibration device as a ridged body (RB) rotated in pitch and roll relative to the level plane (where gravity is normal to this plane). The small table face is placed 90° to the large table face and the last misalignment is the delta between the real angle between the faces and 90°.

The model is a representation of the system with respect to a global frame of reference (G) assigned to the base of the device, which does not contain gravity, meaning that the equations for the system do not change if the RB is rotated in space.

The challenge is to align the system G with the global frame that contains gravity (Gwg). Fortunately, the instrument is referenced to Gwg, so it is possible to use it to assess the calibration device alignment. This latter point is controversial due to the perceived circular nature of this process. Keep in mind that one can use a single-axis inclinometer or bubble level after calibration to align (to level) the very same surface used to calibrate it.

4.0 The Kinematics Model (KM) for the Calibration Device

For the aeronautics community, the established transformation (rotation) matrices in math are not exactly equivalent in terms of the direction of rotation. For instance, positive pitch (α) and yaw (γ) rotations are opposite to the math matrices, while roll or beta does not change.

We use rotation or 3D transformation matrices to describe the system and provide a prefix name for each type of rotation. In this case, *p*rot is for pitch, *r*rot is for roll, and *y*rot is for yaw. To correct for the math transformation vs the aeronautics nomenclature requires changing the sign of the rotation for pitch and yaw.

Math transformation matrices are

$$\text{Pitch rotation, } Ry[\alpha] = \begin{bmatrix} \cos[\alpha] & 0 & \sin[\alpha] \\ 0 & 1 & 0 \\ -\sin[\alpha] & 0 & \cos[\alpha] \end{bmatrix} \tag{8}$$

$$\text{Roll rotation, } Rx[\beta] = \begin{bmatrix} 1 & 0 & 0 \\ 0 & \cos[\beta] & -\sin[\beta] \\ 0 & \sin[\beta] & \cos[\beta] \end{bmatrix} \tag{9}$$

$$\text{Yaw rotation, } Rz[\gamma] = \begin{bmatrix} \cos[\gamma] & -\sin[\gamma] & 0 \\ \sin[\gamma] & \cos[\gamma] & 0 \\ 0 & 0 & 1 \end{bmatrix} \quad (10)$$

Therefore, the system model uses,

1. Pitch rotation, $p\text{rot}[p] = Ry[-p]$
2. Roll rotation, $r\text{rot}[r] = Rx[r]$
3. Yaw rotation, $y\text{rot}[y] = Rz[-y]$

We can use these transformation/rotation matrices to derive the model for the calibration device. First, let us describe the real or physical system. Figure 4 shows all of the misalignments in the real two-axis rotary device described above.

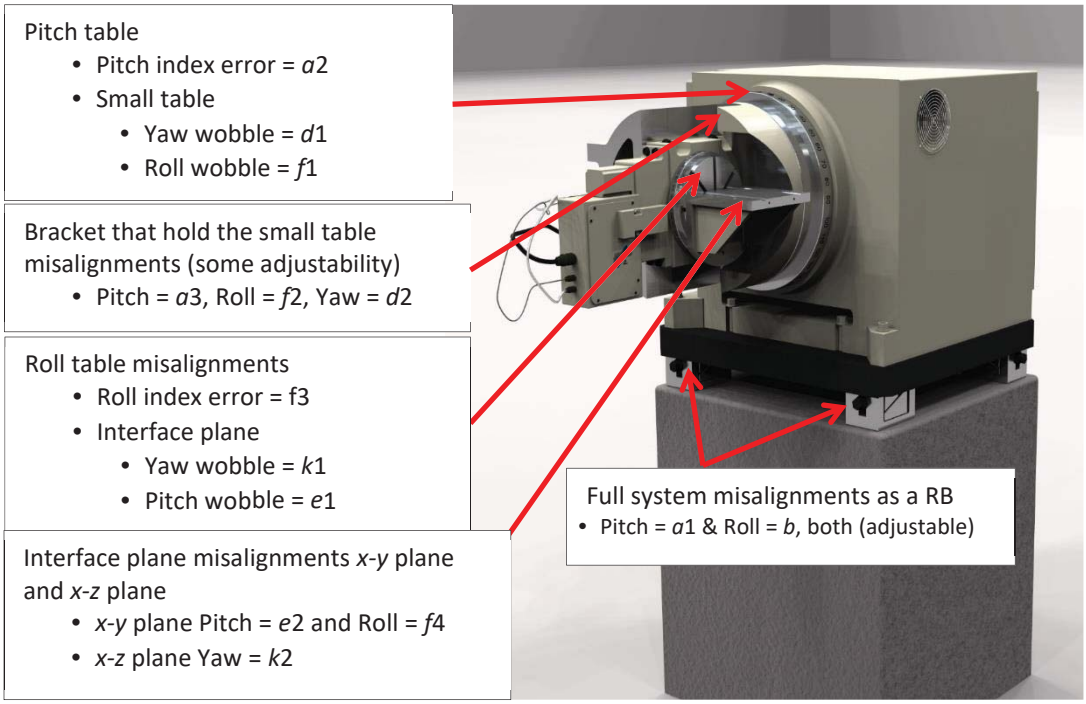

Figure 4: The two-axis divider head calibration system. All 14 misalignments are shown, but if you take the interface plane 3 misalignment and multiply by 4 (one for each mounting orientation, then the number of misalignments increases to 23.

The kinematics model (KM) for this system comes from multiplying the following rotation matrices in the specified order [7]:

$$KM = r\text{rot}[b].p\text{rot}[p].p\text{rot}[a].y\text{rot}[d].r\text{rot}[r].r\text{rot}[f].p\text{rot}[e].y\text{rot}[k].y\text{rot}[y_{fb}].r\text{rot}[u_{tb}] \quad (11)$$

Table 1: Describes each misalignment as an Articulation, Orientation, or Misalignment in the calibration device. The last two rows (described in part (B) of Figure 5) refer to the four mounting orientations

Label	Description	Type	Range
b	Roll; rotation of system as an RB	M	<< ±1°
p	Pitch articulation; rotary table	A	360 & 1° inc.
a	Pitch; total pitch misalignment = *a*1 + *a*2 + *a*3	M	<< ± 1°
*a*1	Pitch; rotation of system as an RB	M	<< ± 1°
*a*2	Pitch index error	M	±2 Arcsecs with zero avg.
*a*3	Pitch; roll table alignment with Pitch table	M	<< ±1°
d	Yaw; total yaw misalignment = *d*1 + *d*2	M	<<±1°
*d*1	Yaw wobble induced by pitch table	M	±5 Arcsecs with zero avg.
*d*2	Yaw misalignment between tables	M	<< ± 1°
r	Roll articulation; rotary table	A	360 & 1° inc.
f	Roll; Total roll misalignment of table and reference= *f*1 + *f*2 + *f*3 + *f*4	M	<< ±1°
*f*1	Roll; wobble induced by pitch table	M	±2 Arcsecs with zero avg.
*f*2	Roll; roll table alignment with pitch table	M	<< ±1°
*f*3	Roll; table index error	M	±2 Arcsecs with zero avg.
*f*4	Roll; *x*-*y* plane misalignment relative the roll table	M	<< ± 1°
e	Pitch; total pitch misalignment of reference = *e*1 + *e*2	M	<< ± 1°
*e*1	Pitch; wobble from roll table	M	±2 Arcsecs with zero avg.
*e*2	Pitch; *x*-*y* plane misalignment relative the roll table	M	<< ± 1°
k	Yaw; total yaw misalignment of reference = *k*1 + *k*2	M	<< ± 1°
*k*1	Yaw; wobble from roll table	M	±2 Arcsecs with zero avg.
*k*2	Yaw; *x*-*y* plane misalignment relative the roll table	M	<< ± 1°
y_{fb}	Orientation of the instrument with respect to one side of the *x*-*y* plane, either forward or backward mount	O	*y* = 0 forward *y* = 180 backward mount
u_{tb}	Orientation of the instrument with respect to the top or bottom side of the *x*-*y* plane	O	*u* = 0 top & *u* = 180 bottom mount

M = Misalignment, O = Orientation, A = Articulation, inc = Increment, avg = Average

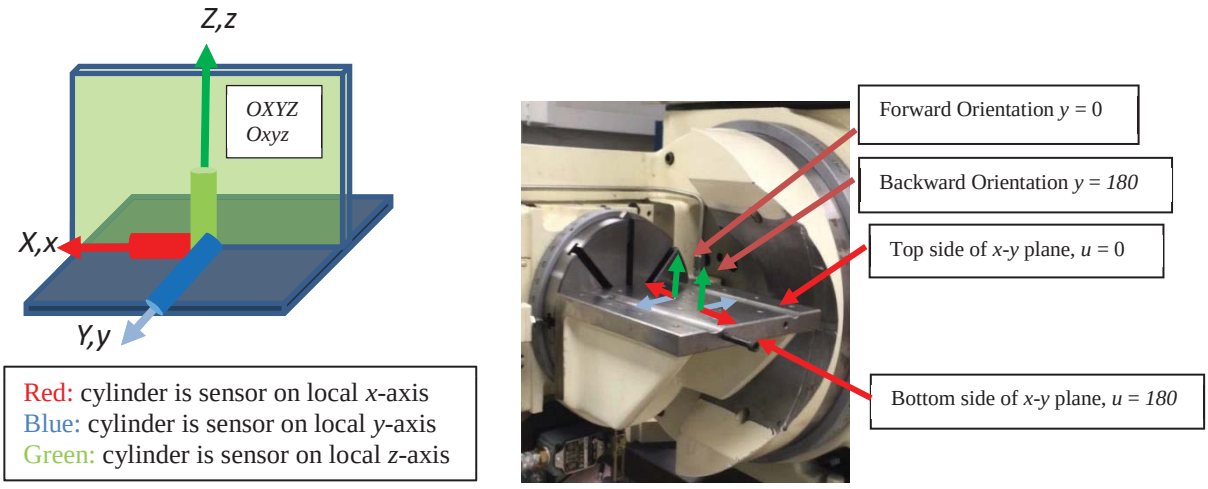

(A) **(B)**

Figure 5: (A) shows the two planes, *x-y* and *x-z* planes that are assigned to the instrument local frame. The goal is to align the instrument local frame (*Oxyz*), which contains the Gwg at this position, to the real or physical *X-Y* and *X-Z* planes of the calibration device G (*OXYZ*). The illustration shows the forward mount, *y* = 0 and top mount *u* = 0. (B) shows two groups of orthogonal axes representing the instrument. The first group represents the orientations *y* = 0 and *u* = 0. The second group represents the orientations *y* = 180 and *u* = 0.

The KM results in a 3x3 matrix where each column vector represents the position of the local 3 axes (*x*, *y*, and *z*) which form the *x-y* and *x-z* planes in the G frame of reference (*X*, *Y*, and *Z*).

$$\begin{matrix} & x & y & z \\ X \\ Y \\ Z \end{matrix} \begin{bmatrix} KM_{1,1} & KM_{1,2} & KM_{1,3} \\ KM_{2,1} & KM_{2,2} & KM_{2,3} \\ KM_{3,1} & KM_{3,2} & KM_{3,3} \end{bmatrix} \tag{12}$$

Technically, this model can represent the instrument if the CD system is in alignment with the Gwg, as expressed in assumption 6. Or stating it differently, the instrument described in this paper is only sensitive to the dot product with the *Z*-axis when it contains the gravity vector (see Figure 3). The third row of the kinematic 3x3 matrix is relevant to this application, and the *x*-axis sensor output corresponds to the *x*.*Z* value, $KM_{3,1}$, the *y*-axis sensor to the *y*.*Z*, $KM_{3,2}$, and *z*-axis sensor to the *z*.*Z* value, $KM_{3,3}$.

5.0 Calibration Procedure

Section 3.1 described the instrument mathematical model $V = B + g_v^T S$. In addition, the approach to obtain the angular attitude of the instrument is $g_v = (V - B)S^{-1}$. In this section, the focus will be obtaining *B* and *S* through a symbolic least square approach [4]. The equation $V = B + g_v^T S$ is rearranged to look like *Ax* = *b* by

$$V = [1 \quad g_v^T] \begin{bmatrix} B^T \\ S \end{bmatrix} <> [1 \quad g_v^T] \begin{bmatrix} B^T \\ S \end{bmatrix} = V \equiv Ax = b \tag{13}$$

where

$$A = [1 \quad g_v^T] = \begin{bmatrix} 1 & g_{x.z_1} & g_{y.z_1} & g_{z.z_1} \\ 1 & g_{x.z_2} & g_{y.z_2} & g_{z.z_2} \\ 1 & g_{x.z_2} & g_{y.z_3} & g_{z.z_3} \\ . & . & . & . \\ . & . & . & . \\ . & . & . & . \\ 1 & g_{x.z_n} & g_{y.z_n} & g_{z.z_n} \end{bmatrix}_{nx4} \tag{14}$$

$$x = \begin{bmatrix} B^T \\ S \end{bmatrix} = \begin{bmatrix} B_x & B_y & B_z \\ S_{xx} & S_{yx} & S_{zx} \\ S_{xy} & S_{yy} & S_{zy} \\ S_{xz} & S_{yz} & S_{zz} \end{bmatrix}_{4x3} \tag{15}$$

and

$$b = V = \begin{bmatrix} Vx_1 & Vy_1 & Vz_1 \\ Vx_2 & Vy_2 & Vz_2 \\ Vx_3 & Vy_3 & Vz_3 \\ . & . & . \\ . & . & . \\ . & . & . \\ Vx_n & Vy_n & Vz_n \end{bmatrix}_{nx3} \tag{16}$$

n is the number of calibration points or articulations used for a calibration.

$$\begin{bmatrix} 1 & g_{x.z_1} & g_{y.z_1} & g_{z.z_1} \\ 1 & g_{x.z_2} & g_{y.z_2} & g_{z.z_2} \\ 1 & g_{x.z_2} & g_{y.z_3} & g_{z.z_3} \\ . & . & . & . \\ . & . & . & . \\ . & . & . & . \\ 1 & g_{x.z_n} & g_{y.z_n} & g_{z.z_n} \end{bmatrix}_{nx4} \begin{bmatrix} B_x & B_y & B_z \\ S_{xx} & S_{yx} & S_{zx} \\ S_{xy} & S_{yy} & S_{zy} \\ S_{xz} & S_{yz} & S_{zz} \end{bmatrix}_{4x3} = \begin{bmatrix} Vx_1 & Vy_1 & Vz_1 \\ Vx_2 & Vy_2 & Vz_2 \\ Vx_3 & Vy_3 & Vz_3 \\ . & . & . \\ . & . & . \\ . & . & . \\ Vx_n & Vy_n & Vz_n \end{bmatrix}_{nx3} \tag{17}$$

$$Ax = b \tag{18}$$

This demonstration requires differentiating from the traditional process [2]. In the traditional calibration, the input (the articulations g_v) is known to some accuracy, and the output of the instrument (*V*) is read for each articulation. For this demonstration, we only know the input to the closest integer. *V* becomes the articulation of the calibration device including the misalignments, g_v, (assumption 9). Borrowing from the single-axis calibration, Figure 1, where the surface level, SL (technically the CD misalignment) is not known, but the sensor output, V, contains SL plus the device internal misalignment (sensor error, e).

To avoid any confusion, ga_v represents the near-known integer value, or $ga_v = g_v$ when all misalignments are 0. Then the instrument output containing the misalignments that pertain to the point is $V = g_v$ for any attitude in space. The new $Ax = b$ will look like

$$\begin{bmatrix} 1 & ga_{x.Z_1} & ga_{y.Z_1} & ga_{z.Z_1} \\ 1 & ga_{x.Z_2} & ga_{y.Z_2} & ga_{z.Z_2} \\ 1 & g_{ax.Z_2} & ga_{y.Z_3} & ga_{z.Z_3} \\ . & . & . & . \\ . & . & . & . \\ . & . & . & . \\ 1 & ga_{x.Z_n} & ga_{y.Z_n} & ga_{z.Z_n} \end{bmatrix}_{nx4} \begin{bmatrix} B_x & B_y & B_z \\ S_{xx} & S_{yx} & S_{zx} \\ S_{xy} & S_{yy} & S_{zy} \\ S_{xz} & S_{yz} & S_{zz} \end{bmatrix}_{4x3} = \begin{bmatrix} g_{x.Z_1} & g_{y.Z_1} & g_{z.Z_1} \\ g_{x.Z_2} & g_{y.Z_2} & g_{z.Z_2} \\ g_{x.Z_2} & g_{y.Z_3} & g_{z.Z_3} \\ . & . & . \\ . & . & . \\ . & . & . \\ g_{x.Z_n} & g_{y.Z_n} & g_{z.Z_n} \end{bmatrix}_{nx3} \quad (19)$$

which is $[1 \quad ga_v^T] \begin{bmatrix} B^T \\ S \end{bmatrix} = g_v = V$.

To obtain $\begin{bmatrix} B^T \\ S \end{bmatrix}$, use the least square method found in Reference 4, which obtains the approximate x or $\tilde{x}$:

$$\tilde{x} = (A^T A)^{-1}(A^T b): \quad (20)$$

$$\begin{bmatrix} B^T \\ S \end{bmatrix} = ([1 \quad ga_v^T]^T [1 \quad ga_v^T])^{-1} [1 \quad ga_v^T]^T g_v \quad (21)$$

To reiterate, the math model shows that the instrument output is a function of the angular articulation of the calibration device, *gv*. This *gv* vector comes from a kinematic math model of a real or physical calibration device, described in Sections 3 and 4. Any physical system that differs from this system will have a different model. The derivation will not be shown, nor how this model was chosen, but the description in Section 4 should provide enough insight to help with any other system. Again, to emulate the calibration of the single-axis instrument, the misalignments in the KM for the calibration device will be set to zero for each angle articulation or as an input for calibration.

The results for the angular attitude of the calibration device to the nearest integer are

- $ga_{x.Z} = x.Z = \sin[p]$;
- $ga_{y.Z} = y.Z = \cos[p] \sin[r]$; and
- $ga_{z.Z} = z.Z = \cos[p] \cos[r]$.

However, the instrument output is equal to the third row of the KM (eq. (11)), which includes the misalignments

- $g_{x.Z} = x.Z = KM[_{3,1}]$; ($KM[_{i,j}]$ = row i, column j);
- $g_{y.Z} = y.Z = KM[_{3,2}]$; and
- $g_{z.Z} = z.Z = KM[_{3,3}]$.

The next step is selecting the calibration points or articulations. The ideal calibration points are the ones that maximize one or more misalignments while minimizing the rest, with each misalignment included in the set. The best positions are those where either pitch or roll are equal to 0° + 90**n*, where *n* = 0, 1, 2, or 3. The system provides 360° in pitch and roll, therefore it is possible to obtain 16 points, shown in Table 2, for each mounting orientation, shown in Table 3.

Table 2: Selected articulations to maximize one or more misalignments while minimizing the others.

p	**0**	**0**	**0**	**0**	**90**	**90**	**90**	**90**	**180**	**180**	**180**	**180**	**270**	**270**	**270**	**270**
r	0	90	180	270	0	90	180	270	0	90	180	270	0	90	180	270

If the system had zero misalignments, then these 16 points would be sufficient to perform a calibration. However, when this is not the case, then it may require additional mounting orientations. A few examples (Section 6) will clarify this issue. The combination of the four mounting orientations defined by y_{fb} and u_{tb} parameters (Table 3) will use all 64 possible points.

Table 3: Values of the 4 possible Orientations.

y	**0**	**Pi**	**0**	**Pi**
u	0	0	Pi	Pi

The following examples will show how to find symmetry in the system for only a few of the misalignments. The next section will demonstrate the impact of each individual misalignment to the instrument coefficient matrix. Combinations of two or more misalignments are obtainable, but due to the large number of these combinations, only a selected few are demonstrated in this paper. The rest of them can be obtain in a similar fashion.

6.0 Examples

The following examples will demonstrate how to obtain the symmetrical counterpart for three individual misalignments. Each example will start with the initial position of the CD at zero pitch and roll and the instrument will be mounted on the top ($u = 0$) of the x-y plane and forward ($y = 0$).

6.1 Example 1

The first example (Figure 6) shows the pitch misalignment of the calibration device as a ridged body, RB, equal to $a1$, with all others equal to 0. The total pitch misalignment a is equal to $a1 + a2 + a3$, where $a2$ has a zero average for any of the sets, and $a3$ can be zeroed by adjusting $a1$. Then the total misalignment, a, will approximate the value $a1$.

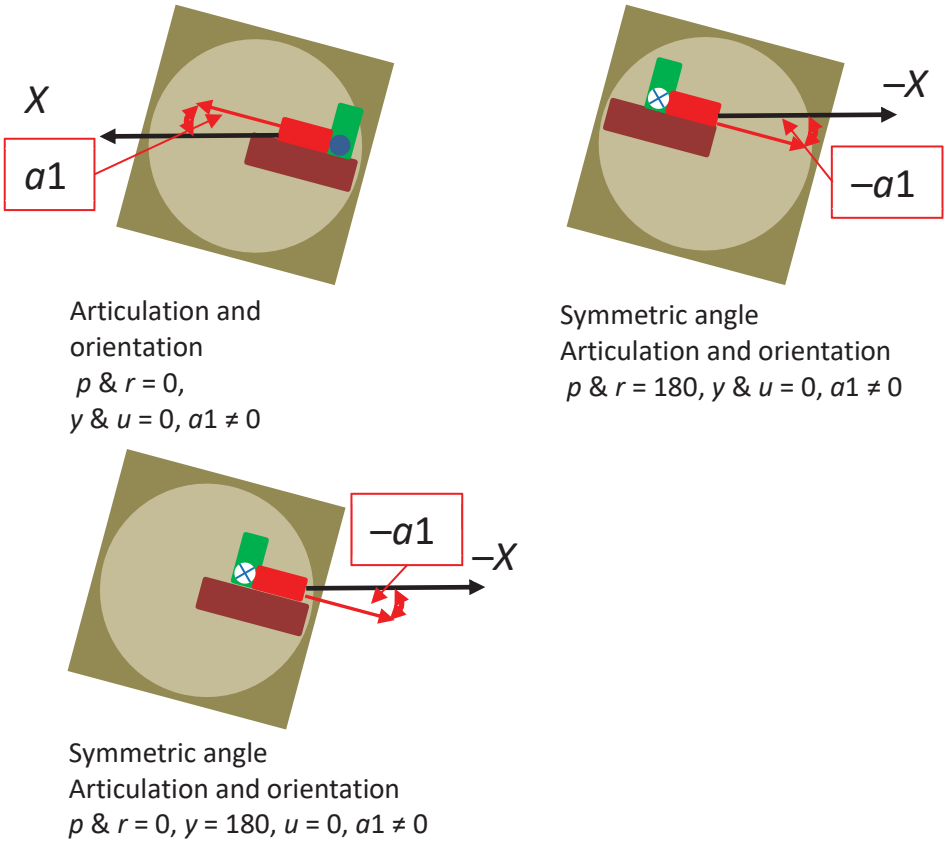

Figure 6: A pitch misalignment of the full system will have two symmetric counterparts. One at *p* & *r* = 180 and the second at *p* & *r* = 0 and *y* = 180. For *u* = 180 (under mount), this creates another set which should be identical to the first if the different mounting orientations are not variable.

6.2 Example 2

The second example (Figure 7) shows the mounting surface, pitch misalignment, or the *x*-*y* plane interface plane, *e*2. The variable misalignment *e*1 has a zero average for any of the sets mentioned in Section 5. The symmetrical point for this misalignment is obtained by rotating the instrument with respect to the normal vector to the *x*-*y* plane, or *y* = 180 in the model.

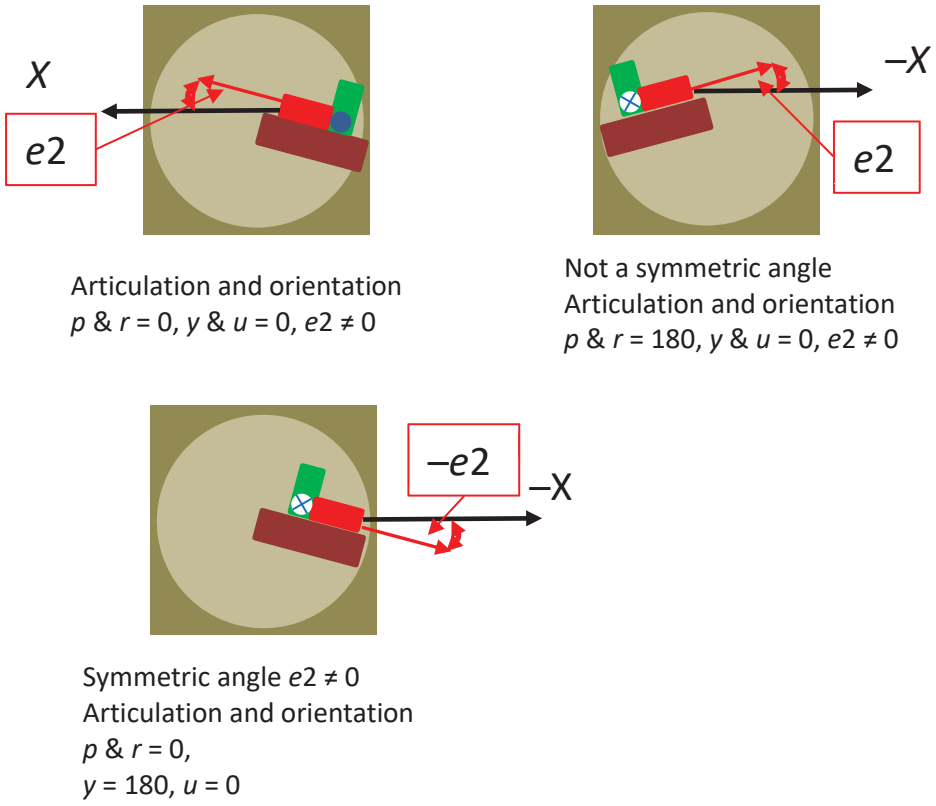

Figure 7: The pitch misalignment of the *x-y* interface plane will have only one symmetric counterpart at *p* & *r* = 0 and *y* = 180. Other pairs of symmetrical counterparts exist at p & r = 180 and when *u* = 180 (mounted under the *x-y* plane) is used for these points.

6.3 Example 3

The last example (Figure 8) shows the dowel holes, yaw misalignment, or the *x-z* plane rotation with respect to the normal vector to the *x-y* plane, *k*2. To obtain the symmetrical angle (-k2) requires placing the instrument on the opposite (bottom) side of the *x-y* plane in either a forward or backward orientation. It is preferable to use the backward orientation since it uses the same side of the dowels; Section 7.6 will expand on this.

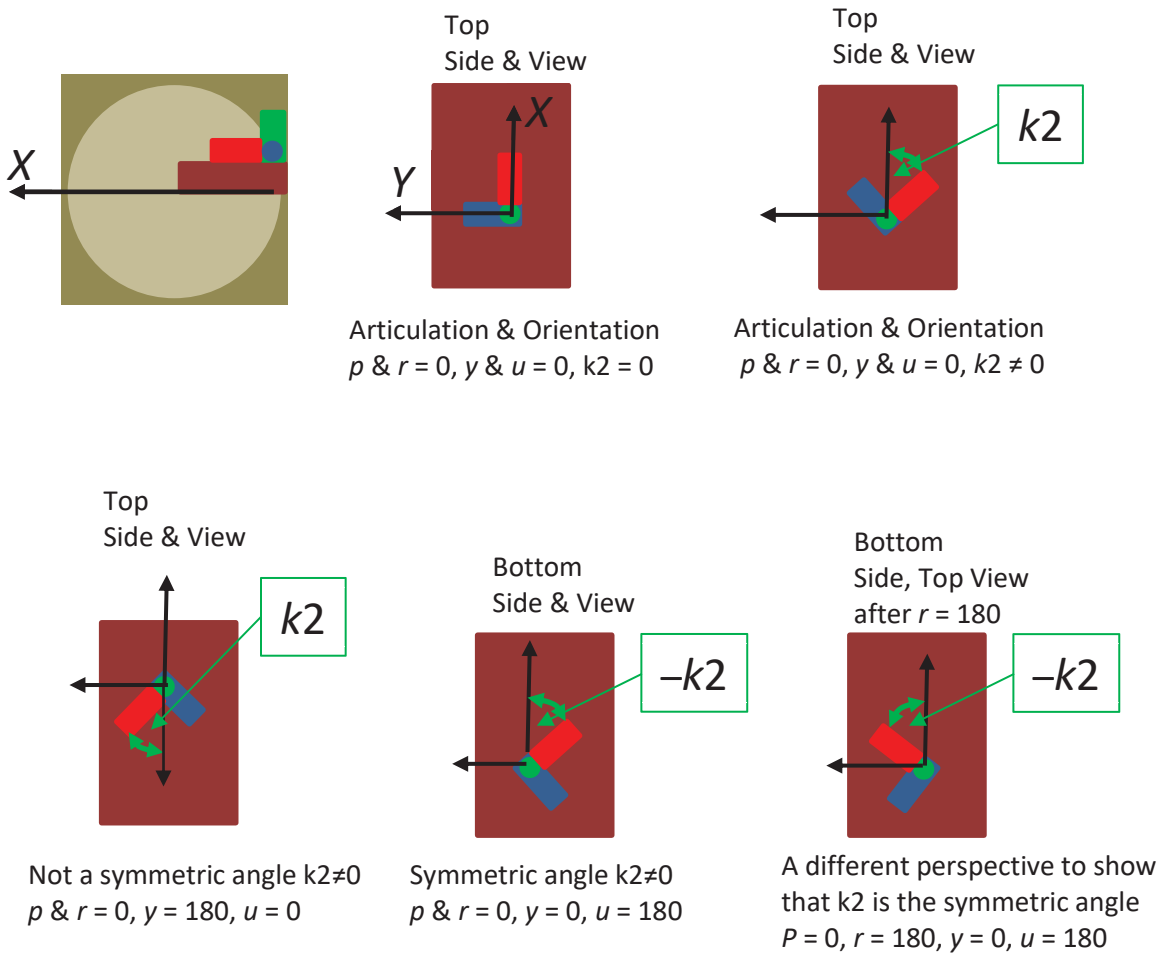

Figure 8: A yaw misalignment of the *x-z* interface plane has only two symmetric point and no other. Using *p*, *r*, y, & u = 0 as the first point, and *p*, *r* & y= 0, & u =180 or *p* & *r* = *0*, and y & u = 180, preferred, as the symmetrical counterpoint.

7.0 Calibration Results

The desired result when calibrating the ideal instrument is to not bias it to the calibration device. The biases will show in the instrument coefficient matrix obtained from the calibration. In practice, the coefficients are not known after assembling the real physical instrument. Therefore, it is hard to determine if the calibration has or has not biased the instrument. In addition, a real instrument will have all of the coefficients in the matrix populated with non-zero values and the sensitivity for the diagonal coefficients will not equal 1. For more on this see Reference 2.

Even for an ideal instrument, the results from a calibration may have the entire coefficient matrix populated with non-zero values, as shown on the left side of Equation 22. The goal is to obtain a result nearly identical to the matrix on the right for the ideal instrument.

$$\underset{\text{calibration}}{\text{Results from}} \begin{bmatrix} Bx & By & Bz \\ Sxx & Syx & Szx \\ Sxy & Syy & Szy \\ Sxz & Syz & Szz \end{bmatrix} \cong \underset{\text{calibration}}{\text{Ideal Instrument}} \begin{bmatrix} 0 & 0 & 0 \\ 1 & 0 & 0 \\ 0 & 1 & 0 \\ 0 & 0 & 1 \end{bmatrix} \tag{22}$$

The first row of the 4X3 matrix is the bias of the sensors, which approximates zero. The diagonal elements of the lower 3x3 matrix, sensor sensitivity, will approximate one. The off diagonal elements of this lower matrix will approximate zero.

A demonstration of a few calibrations of the 3xAI using the CD described in Sections 3 and 4 when one or a combination of misalignments exist in the system is shown below.

7.1 Calibration Example #1

Start with the CD as a RB rotated in pitch with respect to the global frame of reference; *a* (equals *a*1 + *a*2 + *a*3).

To minimize this misalignment, one can use any one set of the 16 points mentioned in Table 2; as we know from the first example in Section 6, no other orientation is required (see Section 6.1) to obtain symmetry. The result is

$$\begin{bmatrix} Bx & By & Bz \\ Sxx & Syx & Szx \\ Sxy & Syy & Szy \\ Sxz & Syz & Szz \end{bmatrix} \cong \begin{bmatrix} 0 & 0 & 0 \\ \cos[a] & 0 & 0 \\ 0 & \cos[a] & 0 \\ 0 & 0 & \cos[a] \end{bmatrix} \tag{23}$$

Using a Taylor expansion, $\cos(a) = 1 - \frac{a^2}{2} + \frac{a^4}{24}$; therefore, when *a* is small in value, then $\cos[a] \cong 1$

The same result is found for the system roll, b, misalignment of the CD as a RB.

7.2 Calibration Example #2

If the CD has an orthogonal misalignment, (*d* = *d*1 + *d*2), when using only one set of points, the result is

$$\begin{bmatrix} Bx & By & Bz \\ Sxx & Syx & Szx \\ Sxy & Syy & Szy \\ Sxz & Syz & Szz \end{bmatrix} \cong \begin{bmatrix} 0 & 0 & 0 \\ \cos[d] & 0 & 0 \\ 0 & 1 & 0 \\ 0 & 0 & 1 \end{bmatrix} \tag{24}$$

This orthogonal misalignment only affects the pitch sensor since the other two sensors stay on the same plane; therefore, they are not affected by this misalignment.

7.3 Calibration Example #3

The next three results are for the interface planes, or the *x*-*y* and *x*-*z* planes.

The pitch misalignment of the *x*-*y* plane is represented by $e = e1 + e2$. To minimize this misalignment, use one set of 16 points (e.g., $y = 0$) and a second set of 16 points after rotating the instrument 180° with respect to the first *x*-*y* plane side used ($y = 180$,) (see Section 6.2). This is identical to the procedure described for the single-axis instrument, Figure 1.

$$\begin{bmatrix} Bx & By & Bz \\ Sxx & Syx & Szx \\ Sxy & Syy & Szy \\ Sxz & Syz & Szz \end{bmatrix} \cong \begin{bmatrix} 0 & 0 & 0 \\ \cos[e] & 0 & 0 \\ 0 & 1 & 0 \\ 0 & 0 & \cos[e] \end{bmatrix} \tag{25}$$

A pitch misalignment only affects the sensors in the *x*-*z* plane (red and green sensors, as shown in Figures 3 and 5). The *y*-axis sensor (blue) does not experience any change for this misalignment. Similarly, if the misalignment of the *x*-*y* plane is a roll angle (*f*) then one can use the same sets for the previous pitch misalignment, section 8.3.1.

$$\begin{bmatrix} Bx & By & Bz \\ Sxx & Syx & Szx \\ Sxy & Syy & Szy \\ Sxz & Syz & Szz \end{bmatrix} \cong \begin{bmatrix} 0 & 0 & 0 \\ 1 & 0 & 0 \\ 0 & \cos[f] & 0 \\ 0 & 0 & \cos[f] \end{bmatrix} \tag{26}$$

A roll misalignment only affects the sensors in the *y*- and *z*-axes (blue and green sensors, as shown in Figures 3 and 5). The *x*-axis sensor (red) does not sense this misalignment.

The yaw misalignment of the *x*-*z* plane with respect to the *X*-axis of the calibration device is $k = k1 + k2$. It can be minimized with one set of 16 points on one side of the *x*-*y* plane (e.g., the top side or $u = 0$) and a second set on the opposite side (i.e., the bottom side or $u = \text{pi}$) of this plane with the same or opposite (preferred) orientation on the underside (see Section 6.3).

$$\begin{bmatrix} Bx & By & Bz \\ Sxx & Syx & Szx \\ Sxy & Syy & Szy \\ Sxz & Syz & Szz \end{bmatrix} \cong \begin{bmatrix} 0 & 0 & 0 \\ \cos[k] & 0 & 0 \\ 0 & \cos[k] & 0 \\ 0 & 0 & 1 \end{bmatrix} \tag{27}$$

This yaw misalignment only affects the two sensors in the *x*-*y* plane (red and blue sensors, as shown in Figures 3 and 5). The *z*-axis sensor output does not change during this misalignment. This misalignment is equivalent to rotating the instrument with respect to the global *Z*-axis when the sensor is in the zero pitch and roll articulation. The correct way to describe it is by rotating the instrument with respect to the local *z*-axis of the instrument, when no other misalignments exist.

7.4 Calibration Example #4

If the system contains two or more misalignments, and depending on which ones, this may drive the number of orientations (*y*&*u*) needed up from one to four orientations. This is due to the compounding of the angles, but specifically to finding the symmetric counterpoints.

7.4.1 *The combination of a pitch (***a***) and roll (***b***)*

For example, the combination of a pitch (*a*) and roll (*b*) of the device as a ridged body only requires any one set of 16 points to minimize them:

$$\begin{bmatrix} 0 & 0 & 0 \\ \cos[a]\cos[b] & 0 & 0 \\ 0 & \cos[a]\cos[b] & 0 \\ 0 & 0 & \cos[a]\cos[b] \end{bmatrix} \tag{28}$$

7.4.2 *The combination of a pitch (***a***), roll (***b***), and yaw (d)*

If you add the orthogonal misalignment, *d*, then it requires a second set of points with a different orientation. If you start with *y* = 0 and *u* = 0, then the second set could be either *y* = 180 and *u* = 0 or *y* = 180 and *u* = 180.

If the misalignments are small, e.g., around 3 arcsecs, then $\mathrm{Cos}[3\ \mathrm{arcsecs}] = 0.999999999894 \cong 1, \mathrm{Cos}[10\ \mathrm{arcsec}] = 0.999999998825 \cong 1$. As an extreme example, if 10 misalignments with 3 arcs are in the system, then $\mathrm{Cos}^{10}[3\ \mathrm{arcsecs}] = 0.99999999894$; or if 36 arcs or 0.01° are used, then $\mathrm{Cos}^{10}[36\ \mathrm{arcsecs}] = 0.99999984769$. The point here is that $\mathrm{Cos}[s]$when s is small can be approximated to 1 for small compound misalignments of near identical magnitudes.

$$\begin{bmatrix} 0 & 0 & 0 \\ \cos[a]\cos[b]\cos[d] & 0 & 0 \\ 0 & \cos[a]\cos[b] & 0 \\ 0 & 0 & \cos[a]\cos[b] \end{bmatrix} \tag{29}$$

7.4.3 *The combination of a pitch (***a***), roll (***b***), yaw (d), and interface plane roll (f)*

If the roll misalignment of the *x*-*y* plane, *f*, is added to the previous misalignments, then the results are

$$\begin{bmatrix} 0 & 0 & 0 \\ Sxx & 0 & 0 \\ 0 & Syy & 0 \\ 0 & 0 & \mathrm{Szz} \end{bmatrix} \tag{30}$$

Table 4: The diagonal coefficients in Equation (30)

3xAI Coefficients in Equation (30)		
Coefficient	Equation	Approximation
S*xx*	$\mathbf{Cos}[\boldsymbol{a}]\mathbf{Cos}[\boldsymbol{b}]\mathbf{Cos}[\boldsymbol{d}]$	1
S*yy*	$\mathbf{Cos}[\boldsymbol{a}]\mathbf{Cos}[\boldsymbol{b}]\mathbf{Cos}[\boldsymbol{f}] - \mathrm{Cos}[b]\mathrm{Sin}[a]\mathrm{Sin}[d]\mathrm{Sin}[f]$	1
S*zz*	$\mathbf{Cos}[\boldsymbol{a}]\mathbf{Cos}[\boldsymbol{b}]\mathbf{Cos}[\boldsymbol{f}] - \mathrm{Cos}[b]\mathrm{Sin}[a]\mathrm{Sin}[d]\mathrm{Sin}[f]$	1

Using the Taylor series, $\mathrm{Sin}(a) = a - \frac{a^3}{6}$. Therefore, the Sin function can be approximated to (a), and if (a) is very small, e.g., 3 arcsecs or 14.5 urads, and if the other misalignments in the system have similar value, the result is 14.5 urads^3 ≅ 3 frads (femto or 10^{-15} radians) or approximate zero for this application. With only two misalignments, the results are in the 10^{-10} radians, which can also be approximated to zero.

7.5 Calibration Example #5

For the following condition where the system contains all of the misalignments, shown in Table 1, and the calibration is performed with only one mount and one set of articulations, the result is

$$\begin{bmatrix} Bx & By & Bz \\ Sxx & Syx & Szx \\ Sxy & Syy & Szy \\ Sxz & Syz & Szz \end{bmatrix} \tag{31}$$

Table 5: Coefficients for First Column in Equation (31)

x-axis Sensor (Red sensor)		
Coefficient	Equation	Approximation
Bx	$-\mathrm{Cos}[e]\mathrm{Cos}[k]\mathrm{Sin}[b]\mathrm{Sin}[d]$	0
Sxx	$\boldsymbol{\mathrm{Cos}[a]\mathrm{Cos}[b]\mathrm{Cos}[d]\mathrm{Cos}[e]\mathrm{Cos}[k]}$	1
Sxy	$-\mathrm{Cos}[b]\mathrm{Cos}[f]\mathrm{Cos}[k]\mathrm{Sin}[a]\mathrm{Sin}[d]\mathrm{Sin}[e]$ $-\mathrm{Cos}[a]\mathrm{Cos}[b]\mathrm{Cos}[k]\mathrm{Sin}[e]\mathrm{Sin}[f]$ $\boldsymbol{-\mathrm{Cos}[a]\mathrm{Cos}[b]\mathrm{Cos}[f]\mathrm{Sin}[k]}$ $+\mathrm{Cos}[b]\mathrm{Sin}[a]\mathrm{Sin}[d]\mathrm{Sin}[f]\mathrm{Sin}[k]$	–k
Sxz	$\boldsymbol{\mathrm{Cos}[a]\mathrm{Cos}[b]\mathrm{Cos}[f]\mathrm{Cos}[k]\mathrm{Sin}[e]}$ $-\mathrm{Cos}[b]\mathrm{Cos}[k]\mathrm{Sin}[a]\mathrm{Sin}[d]\mathrm{Sin}[e]\mathrm{Sin}[f]$ $-\mathrm{Cos}[b]\mathrm{Cos}[f]\mathrm{Sin}[a]\mathrm{Sin}[d]\mathrm{Sin}[k]$ $-\mathrm{Cos}[a]\mathrm{Cos}[b]\mathrm{Sin}[f]\mathrm{Sin}[k]$	e

Table 6: Coefficients for Second Column in Equation (31)

y-axis Sensor (Blue sensor)		
Coefficient	Equation	Approximation
By	$-\mathrm{Cos}[e]\mathrm{Sin}[b]\mathrm{Sin}[d]\mathrm{Sin}[k]$	0
Syx	$\mathbf{Cos}[\boldsymbol{a}]\ \boldsymbol{Cos}[\boldsymbol{b}]\ \mathbf{Cos}[\boldsymbol{d}]\ \mathbf{Cos}[\boldsymbol{e}]\ \mathbf{Sin}[\boldsymbol{k}]$	k
Syy	$\mathbf{Cos}[\boldsymbol{a}]\mathbf{Cos}[\boldsymbol{b}]\mathbf{Cos}[\boldsymbol{f}]\mathbf{Cos}[\boldsymbol{k}] - \mathrm{Cos}[b]\mathrm{Cos}[k]\mathrm{Sin}[a]\mathrm{Sin}[d]\mathrm{Sin}[f] - \mathrm{Cos}[b]\mathrm{Cos}[f]\mathrm{Sin}[a]\mathrm{Sin}[d]\mathrm{Sin}[e]\mathrm{Sin}[k] - \mathrm{Cos}[a]\mathrm{Cos}[b]\mathrm{Sin}[e]\mathrm{Sin}[f]\mathrm{Sin}[k]$	1
Syz	$\mathrm{Cos}[b]\mathrm{Cos}[f]\mathrm{Cos}[k]\mathrm{Sin}[a]\mathrm{Sin}[d] + \mathbf{Cos}[\boldsymbol{a}]\mathbf{Cos}[\boldsymbol{b}]\mathbf{Cos}[\boldsymbol{k}]\mathbf{Sin}[\boldsymbol{f}] + \mathrm{Cos}[a]\mathrm{Cos}[b]\mathrm{Cos}[f]\mathrm{Sin}[e]\mathrm{Sin}[k] - \mathrm{Cos}[b]\mathrm{Sin}[a]\mathrm{Sin}[d]\mathrm{Sin}[e]\mathrm{Sin}[f]\mathrm{Sin}[k]$	g

Table 7: Coefficients for Third Column in Equation (31)

z-axis Sensor (Green sensor)		
Coefficient	Equation	Approximation
Bz	$\mathrm{Sin}[b]\mathrm{Sin}[d]\mathrm{Sin}[e]$	0
Szx	$-\mathbf{Cos}[\boldsymbol{a}]\mathbf{Cos}[\boldsymbol{b}]\mathbf{Cos}[\boldsymbol{d}]\mathbf{Sin}[\boldsymbol{e}]$	–e
Szy	$-\mathrm{Cos}[b]\mathrm{Cos}[e]\mathrm{Cos}[f]\mathrm{Sin}[a]\mathrm{Sin}[d] - \mathbf{Cos}[\boldsymbol{a}]\mathbf{Cos}[\boldsymbol{b}]\mathbf{Cos}[\boldsymbol{e}]\mathbf{Sin}[\boldsymbol{f}]$	–g
Szz	$\mathbf{Cos}[\boldsymbol{a}]\mathbf{Cos}[\boldsymbol{b}]\mathbf{Cos}[\boldsymbol{e}]\mathbf{Cos}[\boldsymbol{f}] - \mathrm{Cos}[b]\mathrm{Cos}[e]\mathrm{Sin}[a]\mathrm{Sin}[d]\mathrm{Sin}[f]$	1

The results shown in bold letters are the dominant components for each coefficient. All of the coefficients are populated, and if you use the approximation mentions above for the sin(*x*), you may find a result as follows:

$$\begin{bmatrix} -\mathrm{Cos}[e]\mathrm{Cos}[k]\mathrm{Sin}[b]\mathrm{Sin}[d] & -\mathrm{Cos}[e]\mathrm{Sin}[b]\mathrm{Sin}[d]\mathrm{Sin}[k] & \mathrm{Sin}[b]\mathrm{Sin}[d]\mathrm{Sin}[e] \\ \mathrm{Cos}[a]\mathrm{Cos}[b]\mathrm{Cos}[d]\mathrm{Cos}[e]\mathrm{Cos}[k] & \mathrm{Cos}[a]\mathrm{Cos}[b]\mathrm{Cos}[d]\mathrm{Cos}[e]\mathrm{Sin}[k] & -\mathrm{Cos}[a]\mathrm{Cos}[b]\mathrm{Cos}[d]\mathrm{Sin}[e] \\ -\mathrm{Cos}[a]\mathrm{Cos}[b]\mathrm{Cos}[f]\mathrm{Sin}[k] & \mathrm{Cos}[a]\mathrm{Cos}[b]\mathrm{Cos}[f]\mathrm{Cos}[k] & -\mathrm{Cos}[a]\mathrm{Cos}[b]\mathrm{Cos}[e]\mathrm{Sin}[f] \\ \mathrm{Cos}[a]\mathrm{Cos}[b]\mathrm{Cos}[f]\mathrm{Cos}[k]\mathrm{Sin}[e] & \mathrm{Cos}[a]\mathrm{Cos}[b]\mathrm{Cos}[k]\mathrm{Sin}[f] & \mathrm{Cos}[a]\mathrm{Cos}[b]\mathrm{Cos}[e]\mathrm{Cos}[f] \end{bmatrix} \quad (32)$$

Using the engineering approximation, you find

$$\begin{bmatrix} 0 & 0 & 0 \\ 1 & k & -e \\ -k & 1 & -f \\ e & f & 1 \end{bmatrix} \quad (33)$$

The reason for the previous approach is to clarify that, if the engineering approximations were implemented at the individual rotations shown in the kinematics model, then each misalignment may have been deemed unnecessary or approximated to zero.

The main difference when using the four mounting orientations is minimization or elimination of all the identified misalignments. After the next approach, in Section 7.6, an explanation follows

as to why all of these approximations may not hold in a real physical system, calibration device, and instrument.

To minimize all misalignments (*a, b, d, f, e,* and *k described in Table 1*) without using approximations for bias and the off-diagonal coefficients, all four mounting orientations are required. The result is

$$\begin{bmatrix} 0 & 0 & 0 \\ Sxx & 0 & 0 \\ 0 & Syy & 0 \\ 0 & 0 & Szz \end{bmatrix} \tag{34}$$

This is the desired outcome to minimize the impact of the calibration device internal misalignments on the instrument coefficients.

Table 8: Diagonal Coefficients in Equation (34)

3xAI Coefficients		
Coefficient	Equation	Approximation
Sxx	$\mathbf{Cos}[\boldsymbol{a}]\mathbf{Cos}[\boldsymbol{b}]\mathbf{Cos}[\boldsymbol{d}]\mathbf{Cos}[\boldsymbol{e}]\mathbf{Cos}[\boldsymbol{k}]$	1
Syy	$\mathbf{Cos}[\boldsymbol{a}]\mathbf{Cos}[\boldsymbol{b}]\mathbf{Cos}[\boldsymbol{f}]\mathbf{Cos}[\boldsymbol{k}]$ $-\mathrm{Cos}[b]\mathrm{Cos}[k]\mathrm{Sin}[a]\mathrm{Sin}[d]\mathrm{Sin}[f]$ $-\mathrm{Cos}[b]\mathrm{Cos}[f]\mathrm{Sin}[a]\mathrm{Sin}[d]\mathrm{Sin}[e]\mathrm{Sin}[k]$ $-\mathrm{Cos}[a]\mathrm{Cos}[b]\mathrm{Sin}[e]\mathrm{Sin}[f]\mathrm{Sin}[k]$ $=\mathrm{Cos}[a]\mathrm{Cos}[b]\mathrm{Cos}[f]\mathrm{Cos}[k]$	1
Szz	$\mathbf{Cos}[\boldsymbol{a}]\mathbf{Cos}[\boldsymbol{b}]\mathbf{Cos}[\boldsymbol{e}]\mathbf{Cos}[\boldsymbol{f}]$ $-\mathrm{Cos}[b]\mathrm{Cos}[e]\mathrm{Sin}[a]\mathrm{Sin}[d]\mathrm{Sin}[f]$	1

When using the approximation for small cosine angles, then

$$\begin{bmatrix} B^T \\ S \end{bmatrix} = \begin{bmatrix} 0 & 0 & 0 \\ 1 & 0 & 0 \\ 0 & 1 & 0 \\ 0 & 0 & 1 \end{bmatrix} \tag{35}$$

7.6 Considerations for Real Physical Systems

The following are a few notes on the results when considering a real physical system. When comparing the final two calibration examples, it is possible to conclude that there may not be much of a difference between both approaches if the misalignments in the *x-y* and *x-z* planes are small. Keep in mind that we do not know the misalignments in the system and that there is no instrumentation available to estimate them. Therefore, if they do exist, then they have the potential to show up as part of the instrument coefficients, especially after using only one set of 16 points for the calibration, as demonstrated in Table 7. Appendix A demonstrates that it is possible to calibrate with points that can increase the likelihood of this problem, even for an ideal instrument.

This work assumes that the misalignments, which can vary from calibration point to point, specifically the index and wobble variable misalignments, have a random or sinusoidal variation with an average of zero. The real variations for any system may not behave in this fashion;

therefore, the contributions of these variable misalignments may be greater than the outcome presented above. There is an ongoing investigation in this area that will be included in a future paper.

In addition, it is assumed that the different mounting orientations do not provide variation, but the truth is that in a real system, this is the largest source of variation because the calibrator has to take the instrument off and reinstall for the four different orientations. These variations do not have a zero mean, so they will have a large effect on the instrument coefficients. Remember, this is a least square operation, and the fit is always dependent on the data. In fact, it is speculated, based on computational observations, that these variations from mount to mount can bring the three other misalignments (*a*, *b*, and *d described in Table 1*) into play and show up in the coefficient matrix. It is also difficult to model these variations since they can be a combination of the surface, flatness variation, and the instrument's three individual feet (not on the same plane). It is possible for the interface plane between the calibration device and instrument to distort the sensor position relative to each other during installation. In other words, we start with an instrument with non-orthogonal sensors, and this near orthogonal configuration can change from mount to mount. The measurement will vary slightly when fastening the instrument to the object of interest, and this is exacerbated when using different fastening sequences.

There are other factors not considered in this paper that can cause real instrumentation issues, such as temperature effects. The real 3xAI instrument parameters will vary with temperature. The frame that holds the sensors, in a near orthogonal configuration, will move with temperature changes, thus potentially changing the position of the sensors with respect to each other and the two reference planes.

The *x-y* plane of this instrument and of the calibration device will not be flat and smooth, and the alignment of the *x-z* plane on the top and bottom will not have the same orientation. What makes this challenging for the *x-y* plane is the fact that the instrument has a very small footprint. This small footprint makes it susceptible to particle contamination and to surface deformations (non-flat). For the *x-z* plane of the instrument referenced, the two dowels have the potential to introduce variability if they are not normal. Any tilt in these dowels will have an effect for two of the four orientations because it uses two different sides of the dowels during the four orientations.

One note of caution, the demonstration used points that encompass all quadrants of a 3D sphere. The system is capable of providing 360°×360° points. If the points are all on one-half of the sphere when divided vertically (see Figure A.1) then the results will be dependent on the pitch selected. Appendix A will show these results as a separate demonstration.

8.0 Conclusion

The aeronautics community relies on angle measurements during all wind tunnel tests. This measurement is used from model setup to calibrating other wind-on angle measurement devices. One of the most important parameters in aeronautics research is obtaining aircraft drag count. This coefficient is a function of the drag force an aircraft experiences, and this force is a function of the angle. For this reason it is important to calibrate the angle measurement instrument, relative to

gravity, to very high accuracy, since some research labs consider +/- 1 drag count change, when the aircraft is at a cruise angle, to be equivalent to +/- 0.005 degrees with uncertainty angle change. The metrology norm in calibrating a 3xAI instrument requires a calibration device, CD, that can provide known points to an accuracy that is equal to or higher than the instrument accuracy under calibration. For this type of instrument, determining any known point value with respect to the gravity vector is extremely difficult, and trying to estimate the internal misalignments of any CD is even more difficult. What this paper has shown in Section 7.5, is that it is possible to calibrate this specific type of instrument without accurate knowledge of the calibration input angle articulations. The possibility lies in the fact that the system has to meet a number of requirements (Section 2) for this to work plus the additional mounting orientations. One caveat is that even if it does work, there is still the opportunity to introduce some variability due to human interactions and temperature. This paper is just the starting point for the discussion of calibrating such instruments to high accuracy. What is new are the different mounting orientations, especially for $u = 180°$. That configuration was never thought of because there was no means to measure the benefits of doing so for the 3xAI instrument.

The symmetrical counterpart for the *x*-*z* plane was found through simulations at the symbolic level. The desire to understand the impact of the misalignments on an instrument calibration is what drove this symbolic math approach. Achieving the same results computationally may have led to an incorrect solution, because it is difficult to differentiate how these misalignments contribute to each of the instrument coefficients. In addition, there is the temptation to round small angle misalignment down to zero.

Finally, the observation of using only one mount vs four mounts to minimize the misalignment shows the potential for both approaches to provide similar results. This can only be true if the system variations have zero mean, which we have not found to be the case, and the misalignments are very small (smaller than the desired accuracy of the instrument), which we cannot independently verify. Then again, it is nearly impossible to estimate any or all misalignments in the calibration device even with today's state-of-the-art technology.

9.0 References

1. Tripp, J. S. and Tcheng, P., “Uncertainty Analysis of Instrument Calibration and Application," NASA TP-1999-209545, 1999.
2. Peter A. Parker, and Tom D. Finley, “Advancements in Aircraft Model Force and Attitude Instrumentation by Integrating Statistical Methods”, JOURNAL OF AIRCRAFT Vol. 44, No. 2, March–April 2007
3. Marshall, R., and Landman, D., “An Improved Method for Determining Pitch and Roll Angles Using Accelerometers,"21st AIAA Advanced Measurement Technology and Ground Testing Conference, Denver, Colorado, AIAA 2000-2384, June 2000.
4. Strang, G., “Introduction to Linear Algebra," Wellesley Cambridge Press, Chapter 4.3, Fifth Edition
5. Stone, J. A., Amer, M., Faust, B., Zimmerman, J., "Angle metrology using AAMACS and two small-angle measurement systems," Proceeding of SPIE 5190, Recent Developments in Traceable Dimensional Measurements II, November 2003
6. Finley, T. D., “Technique for Calibrating Angular Measurement Devices when Calibration Standards are Unavailable," NASA Technical Memorandum 104148, Hampton, Virginia, August 1991.
7. Jazar, R.N., “Theory of Applied Robotics," Springer, Chapter 2 and 3, Second Edition

Appendix A Calibration result when using only one mount and all points on one side of the sphere

Warning: It is not feasible to provide a set of random articulation points in symbolic form and obtain a closed-form solution. This demonstration will use one point in each quadrant and the relation is that it is the mirror image on the other side of the two global planes (*X*-*Y* and *X*-*Z*):

$$V = [1 \quad g_v^T] \begin{bmatrix} B^T \\ S \end{bmatrix} <> [1 \quad g_v^T] \begin{bmatrix} B^T \\ S \end{bmatrix} = V \equiv Ax = b \tag{A.1}$$

Figure A.1 is a demonstration of what happens when using articulations concentrated on one side (left or right of the yellow plane) of the sphere where pitch is limited to a range above and below the *x*-*y* plane represented in blue. The red plane represent the x-z plane.

Figure A.1: The calibration device can be represented wih a sphere.

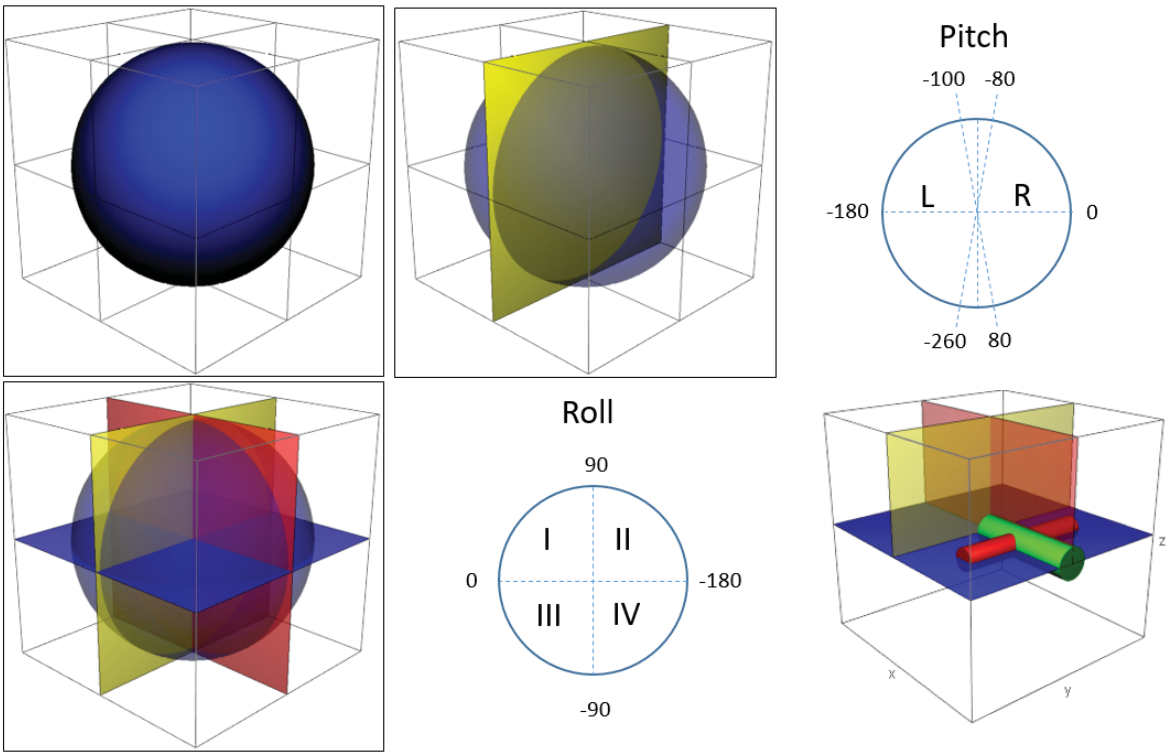

p	-45	-45	-45	-45	45	45	45	45
r	-45	45	135	225	-45	45	135	225

If the sphere is divided by 2 (the yellow plane), then all pitch points will be on the right side or left side of this plane. If you select points on the right or left side within the pitch limits shown above and use only one point per quadrant for roll, they all have to be symmetric relative to the blue plane. With these points, it is possible to show a closed-form solution. For instance, if the choice for pitch and roll is 45°, then the calibration points will be similar to the ones in the above table.

For instance, in Table A.1, the points may seem symmetrical for pitch and roll, but this is not the case.

Table A.1: Resultant g Components for Selected Articulations.

p	**–45**	**–45**	**–45**	**–45**	**45**	**45**	**45**	**45**
r	–45	45	135	225	-45	45	135	225
gx	$-\frac{1}{\sqrt{2}}$	$-\frac{1}{\sqrt{2}}$	$-\frac{1}{\sqrt{2}}$	$-\frac{1}{\sqrt{2}}$	$\frac{1}{\sqrt{2}}$	$\frac{1}{\sqrt{2}}$	$\frac{1}{\sqrt{2}}$	$\frac{1}{\sqrt{2}}$
gy	$-\frac{1}{2}$	$\frac{1}{2}$	$\frac{1}{2}$	$-\frac{1}{2}$	$-\frac{1}{2}$	$\frac{1}{2}$	$\frac{1}{2}$	$-\frac{1}{2}$
gz	$\frac{1}{2}$	$\frac{1}{2}$	$-\frac{1}{2}$	$-\frac{1}{2}$	$\frac{1}{2}$	$\frac{1}{2}$	$-\frac{1}{2}$	$-\frac{1}{2}$

The results from using symmetrical calibration points on one side of the sphere will look like this:

$$\begin{bmatrix} a\,\mathrm{Cos}[p] & a\,k\,\mathrm{Cos}[p] & -a \\ \mathrm{Cos}[a]\mathrm{Cos}[b]\mathrm{Cos}[d]\mathrm{Cos}[e]\mathrm{Cos}[k] & k & -e \\ -e\,b\,\mathrm{Sec}[p]-k & -b\,g\,\mathrm{Sec}[p]+\mathrm{Cos}[a]\mathrm{Cos}[b]\mathrm{Cos}[f]\mathrm{Cos}[k] & -b\,\mathrm{Sec}]p]-f \\ e & b\,\mathrm{Sec}[p]+f & \mathrm{Cos}[e]\mathrm{Cos}[a]\mathrm{Cos}[b]\mathrm{Cos}[f] \end{bmatrix} \quad \text{(A.2)}$$

Approximation using techniques described in section 7, then A.2 becomes A.3

$$\begin{bmatrix} a\,\mathrm{Cos}[p] & a\,k\,\mathrm{Cos}[p] & -a \\ 1 & k & -e \\ -e\,b\,\mathrm{Sec}[p]-k & -b\,f\,\mathrm{Sec}[p]+1 & -b\,\mathrm{Sec}]p]-f \\ e & b\,\mathrm{Sec}[p]+f & 1 \end{bmatrix} \quad \text{(A,3)}$$

These results show that some of the coefficients are dependent on the pitch angle selected. For the bias (*B*) of the sensors, it shows that it is best to select an angle $p = 90°$, but if you do so, then the two coefficients which depend on Sec[p] will go to infinity. In practice, this does not happen because when you attempt to use 90° for pitch, the system is not on either the right or left side of the sphere; therefore, using $p = 90°$ will make the matrices singular. If the midpoint, 45°, is used, then it provides the following result:

$$\begin{bmatrix} a/\sqrt{2} & 0 & -a \\ 1 & k & -e \\ -k & 1 & -(b\sqrt{2}+\mathrm{f}) \\ e & b\sqrt{2}+\mathrm{f} & 1 \end{bmatrix} \quad \text{(A.4)}$$

The results show that the instrument has a nonzero bias, which is a function of the pitch ($a = a1 + a2 + a3$) misalignment. In addition, the coefficients which contained the x-y plane roll misalignment (f) now contains the system roll (b) misalignment. This is similar but not exactly the same result obtained in calibration #5 (section 7.5). On the other hand, if an additional 8 points with symmetrical pitch values (e.g. $p = 135$ and 225) from the other side of sphere are included, e.g. p and r = 45°+ 90°n; n= 1, 2, 3, 4, then the results will match the example #5:

$$\begin{bmatrix} 0 & 0 & 0 \\ 1 & k & -\mathrm{e} \\ -k & 1 & -\mathrm{f} \\ e & \mathrm{f} & 1 \end{bmatrix} \tag{A.5}$$

The intent here is to show the additional bias to the instrument when using points on either the right or left side of the sphere, even when the internal misalignments within the CD are considered small vs using one mount of symmetrical points but using the full sphere with points on both sides of the yellow plane in figure A.1.

Appendix B: Batch processing instrument voltages into g vectors for n number of angle articulations

Here is a linear algebra trick for batch processing. It eliminates the need to subtract the bias from all of the 3 sensor voltages before performing the remaining matrix operations. It makes it easier to perform the math, including spreadsheet software.

For example, the process of obtaining the gravity vector using the new model is

$$g_v = (V - B)^T S^{-1} \tag{B.1}$$

This process requires subtracting *B* from every single *V*. Then you can multiply the result by the inverse of the sensitivity to obtain g_v for a batch of data.

The trick here is to do the following: Add a column of ones to all the voltage output of the instrument for each articulation, and create a matrix with the negative bias on the top row and a 3×3 identity matrix below this row.

$$V_{nx4} = [1 \quad V^T];\ B_{4x3} = \begin{bmatrix} -B^T \\ I \end{bmatrix} = \begin{bmatrix} -B_x & -B_y & -B_z \\ 1 & 0 & 0 \\ 0 & 1 & 0 \\ 0 & 0 & 1 \end{bmatrix};\ S_{3x3}^{-1} = \begin{bmatrix} S_{xx} & S_{yx} & S_{zx} \\ S_{xy} & S_{yy} & S_{zy} \\ S_{xz} & S_{yz} & S_{zz} \end{bmatrix}^{-1} \tag{B.2}$$

The full batch of $g_{v\,nx3} = V_{nx4} B_{4x3} S_{3x3}^{-1}$ can be computed at once.

REPORT DOCUMENTATION PAGE

Form Approved
OMB No. 0704-0188

1. REPORT DATE *(DD-MM-YYYY)*	2. REPORT TYPE	3. DATES COVERED *(From - To)*
08-01-2020	Technical Memorandum	

4. TITLE AND SUBTITLE
Calibrating a 3-Axis Accelerometer Instrument with a Less Accurate Calibration Device Part 1: Mathematical Methodology.

5a. CONTRACT NUMBER

5b. GRANT NUMBER

5c. PROGRAM ELEMENT NUMBER

6. AUTHOR(S)
Hector L Soto

5d. PROJECT NUMBER

5e. TASK NUMBER

5f. WORK UNIT NUMBER
951888.03.07.03.02.01

7. PERFORMING ORGANIZATION NAME(S) AND ADDRESS(ES)
NASA Langley Research Center
Hampton, VA 23681-2199

8. PERFORMING ORGANIZATION REPORT NUMBER

9. SPONSORING/MONITORING AGENCY NAME(S) AND ADDRESS(ES)
National Aeronautics and Space Administration
Washington, DC 20546-0001

10. SPONSOR/MONITOR'S ACRONYM(S)
NASA

11. SPONSOR/MONITOR'S REPORT NUMBER(S)
NASA-TM-2020-5005041

12. DISTRIBUTION/AVAILABILITY STATEMENT
Unclassified-
Subject Category 71
Availability: NASA STI Program (757) 864-9658

13. SUPPLEMENTARY NOTES

14. ABSTRACT
A three-axis accelerometer instrument (3xAI) can provide the angular attitude of a 3D object using the gravity vector (g) as the sole reference. Calibrating such an instrument requires placing it at known (to some accuracy plus uncertainty) angular articulations with respect to g. This paper will show a potential process for calibrating a 3xAI by using a 2-axis rotary system (calibration device) to provide these articulations. Any calibration device (CD) with such capacity will contain internal misalignments. These misalignments, even if made relatively small or approximated to zero in the kinematics model (KM), can be detrimental to the calibration of the instrument when high measurement accuracy is required.

15. SUBJECT TERMS
Angle, tilt, calibration, 3-axis, servo,accelerometer, pitch, roll, yaw, sensor, instrument, accuracy, uncertainty, linear regression, least square, single axis, level, gravity, vector, magnitude, axes, divider head, table, misalignments, offset error, coefficients, bias, sensitivity

16. SECURITY CLASSIFICATION OF:			17. LIMITATION OF ABSTRACT	18. NUMBER OF PAGES	19a. NAME OF RESPONSIBLE PERSON
a. REPORT	b. ABSTRACT	c. THIS PAGE			STI Help Desk (email: help@sti.nasa.gov)
					19b. TELEPHONE NUMBER *(Include area code)*
U	U	U	UU	38	(757) 864-9658